New perspectives on the Li isotopic composition of the upper continental crust and its weathering signature

Lucie Sauzéat, Roberta L Rudnick, Catherine Chauvel, Marion Garçon, Ming Tang

New perspectives on the Li isotopic composition of the upper continental crust and its weathering signature

Lucie Sauzéat[1,2*], Roberta L. Rudnick[1], Catherine Chauvel[2,3], Marion Garçon[4], Ming Tang[1]

[1]*Department of Geology, University of Maryland, College Park, MD 20742, USA*

[2]*University of Grenoble Alpes, ISTerre, F-38041 Grenoble, France*

[3]*CNRS, ISTerre, F-38041 Grenoble, France*

[4]*Carnegie Institution of Washington, Department of Terrestrial Magnetism, Washington, DC 20015, USA*

*correspondence: lucie.sauzeat@ens-lyon.fr

Abstract

Lithium isotopes are increasingly used to trace both present-day and past weathering processes at the surface of the Earth, and could potentially be used to evaluate the average degree of past weathering recorded by the upper continental crust (UCC). Yet the previous estimate of average δ^7Li of the UCC has a rather large uncertainty, hindering the use of Li isotopes for this purpose. New δ^7Li for desert and periglacial loess deposits (windblown dust) from several parts of the world (Europe, Argentina, China and Tajikistan) demonstrate that the former are more homogeneous than the latter, and may therefore serve as excellent proxies of the average composition of large tracts of the UCC. The Li isotopic compositions and concentrations of desert loess samples are controlled by eolian sorting that can be quantified by a binary mixing between a weathered, fine-grained end-member, dominated by phyllosilicates and having low δ^7Li, and an unweathered, coarse-grained end-member, that is a mixture of quartz and plagioclase having higher δ^7Li. We use correlations between insoluble elements (REE, Nd/Hf and Fe_2O_3/SiO_2), Li concentrations (henceforth referred as [Li]), and δ^7Li to estimate a new, more precise, average Li isotopic composition and concentration for the UCC: [Li] = 30.5 ± 3.6

(2σ) ppm, and δ^7Li = +0.6 ± 0.6 (2σ). The δ^7Li for desert loess deposits is anti-correlated with the chemical index of alteration (CIA). Using this relationship, along with our average δ^7Li, we infer that (1) the present-day CIA of the average UCC is 61^{+4}_{-2} (2σ), higher than the common reference value of 53, and (2) the average proportion of chemically weathered components is as high as 37^{+17}_{-10} (2σ) % at the surface of the Earth.

Keywords: *Li isotopes, loess, upper continental crust, chemical weathering*

1. Introduction

Weathering is an ubiquitous process that occurred in the past to form (meta-)sedimentary rocks ("past weathering") and still occurs at present to create sediments and soils ("present-day weathering"). It shapes the continental crust and modifies its chemical composition by producing detrital sediments and releasing ions into the hydrosphere over geological timescales (Taylor and McLennan, 1985; Rudnick, 1995; Lee et al., 2008; Liu and Rudnick, 2011). Chemical weathering also indirectly controls the evolution of climate because carbonates, precipitating with Ca released during weathering of the continental crust, sequester CO_2 (Gaillardet et al., 1999; Amiotte-suchet et al., 2003; Jin et al., 2014). Constraining the degree of weathering experienced by the uppermost part of the crust in the past is thus important in providing a framework that can be used to understand both the compositional evolution of the upper crust and climate variation through time.

It is now well established that lithium isotopes are fractionated by low-temperature processes due to preferential partitioning of ^{7}Li (the heavy isotope) into water while ^{6}Li (the light isotope) is incorporated into the weathered products of silicate rocks such as clays (e.g., Pistiner and Henderson, 2003; Vigier et al., 2008). Li isotopes are thus excellent tracers of fluid-rock reactions and have been used to trace weathering processes (Kısakürek et al., 2005; 2004; Liu et al., 2013; Millot et al., 2010; Rudnick et al., 2004), estimate the mass of continental crust lost

by chemical weathering through geological times (i.e., Li dissolved in river water) (Liu and Rudnick, 2011) and constrain the present-day erosion cycle of mountain ranges (Dellinger et al., 2014). In addition, Li isotopes are not significantly fractionated by high-temperature processes such as metamorphic dewatering (Qiu et al., 2011; 2009; Teng et al., 2007) or igneous differentiation (Teng et al., 2006; Tomascak et al., 1999), hence they are also useful proxies for studying crustal recycling in subduction zones (Elliott et al., 2006; Tang et al., 2014) or beyond (e.g., Vastelic et al., 2011). Here, we propose to use Li isotopes to quantify the importance of chemical weathering experienced by the upper crust in the past.

To date, the published average lithium concentrations for the upper continental crust differ by more than 40%, ranging from 20 ppm (Taylor and McLennan, 1985) to more than 40 ppm (Teng et al., 2004; Hu and Gao, 2008). The average Li isotopic composition of the UCC (δ^7Li = 0 ± 4 (2σ, Teng et al., (2004)) is estimated to be lower than that of fresh, mantle-derived basalts, suggesting that the upper crust records a weathering signature, but the uncertainty on this value overlaps with that of the mantle (δ^7Li ≈ +4 ± 2 (2σ), average derived from Chan et al. 1992, Seitz et al., 2004, and Tomascak et al., 2008).

In this paper, we report [Li] and δ^7Li for loess deposits that sample vast regions of the UCC. The main advantage of using loesses instead of other sediments (e.g., shales, mudrocks, etc.) for this purpose is that loesses are deposits of eolian dust produced by mechanical erosion and mixing of silt derived from glacial outwash and/or desert environments (Pye, 1995); thus they generally experienced little chemical weathering during their formation. These two features allow loess deposits to be considered as proxies for the average UCC composition (Chauvel et al., 2014; Gallet et al., 1996; 1998; McLennan, 2001; Peucker Ehrenbrink and Jahn, 2001; Taylor et al., 1983).

2. Samples

Loess samples cover about 10% of the Earth's surface (Haase et al., 2007; Pécsi, 1990) and

formed between the end of the Pliocene and the beginning of the Pleistocene, based on thermoluminescence dating (Liu, 1985). These Quaternary deposits can be divided into two distinct types: (1) periglacial loess, derived from glacial outwash and transported by winds over limited distances (Haase et al., 2007; Rousseau et al., 2014), and (2) desert loess, transported over longer distances, typically several hundreds of kilometers (Ding et al., 1999), from desert regions.

In this study, we analyzed previously well-characterized desert loesses from China (Jixian, Xifeng, Xining and Luochuan) (Gallet et al., 1996; Jahn et al., 2001), Tajikistan (Chashmanigar) (Ding et al., 2002; Yang et al., 2006) and Argentina (Buenos Aires) (Gallet et al., 1998), as well as periglacial loesses from Western Europe (France, England) and Spitsbergen (Gallet et al., 1998). A map showing the sample locations can be found in Chauvel et al. (2014). Mineralogy, provenance and grain-size distribution for these deposits have been reported in previous studies such as Jeong et al. (2008) and Bronger and Heinkele (1990) for the mineralogy of the Chinese loesses, Smith et al. (2003) and Zarate et al. (2003) for the source location of the Argentinian loesses, and Ding and Ding, (2003) for the grain-size distribution of loesses from Tajikistan.

3. Methods

3.1. Major, trace elements, and radiogenic isotopes

Trace element concentrations and Nd-Hf isotopes have been previously published for all the loess samples (Chauvel et al., 2014; Gallet et al., 1996). Major element concentrations are available in the literature for most of the samples (Gallet et al., 1998; 1996; Jahn et al., 2001), except for the Tajikistan loesses. We thus analyzed their major element contents in this study (see Supplementary Table A).

Major element data for the Tajikistan samples were determined using an ICP-AES (Varian 720 ES) at ISTerre (Grenoble) following the same procedure described in Chauvel et al. (2011); only a brief synopsis is provided here. About 50 mg of powder, hand-crushed in an agate mortar were

dissolved in a HF-HNO_3 mixture in Savillex beakers for about 72 h at 90°C. Boric acid was added to neutralize the HF and the resulting liquid was diluted with milliQ water. The concentrations are calculated using calibration curves based on diluted and doped (Al, Mg, Ca, Na, K and P) BCR-2 rock standard solutions.

Both accuracy and reproducibility of the major element contents of loesses from Tajikistan were monitored by replication of international rock standards. The concentrations obtained for the rock standards are in agreement with the reference values, and reproducibility is, on average, better than 5% (2σ) (see Supplementary Table B).

3.2. Lithium isotopic compositions

Lithium isotopic compositions were measured at the University of Maryland. For each sample, about 25 mg of rock powder was dissolved in a Savillex screw-top beaker in an HF-HNO_3 mixture following the procedure detailed by Teng et al. (2004). For samples containing organic matter, a second step of dissolution using a combination of HF-HNO_3-$HClO_4$ was employed to achieve a complete digestion. Separation of lithium was performed by chromatography on four successive columns following the ion resin techniques described by Moriguti and Nakamura (1998a). Lithium was purified using columns filled with 1 ml of Bio-Rad AG 50w-x12 (200–400 mesh) resin, first with an HCl solution, followed by an HCl-ethanol mixture. Lithium isotopic composition of the purified solutions (~50 ppb Li in 2% HNO_3) were measured on a Nu Plasma Multicollector Inductively Coupled Plasma Mass Spectrometry (MC-ICPMS) and calculated by standard bracketing using L-SVEC (Flesch et al., 1973) as the reference standard. Prior to each analysis, the Na/Li ratio of the solution was determined and samples with Na/Li ratio greater than 5 went through further purification by chromatography.

The accuracy of the Li isotopic composition is assessed based on the analysis of two rock reference materials (AGV-1 and G-2). Our measured values (Supplementary File A and Supplementary Table C) are within uncertainty of previously published results, with $\delta^7Li_{AGV\text{-}1}$=

+6.7 ± 0.7 (2σ, n=3), versus +4.6 to +6.7 (Liu et al., 2013; 2010; 2015; Magna et al., 2004), and $\delta^7Li_{G\text{-}2}$ = +0.6 ± 1.8 (2σ, n=3) versus -1.6 to +2.2; (James and Palmer, 2000; Liu et al., 2010; Pistiner and Henderson, 2003; Tang et al., 2014). The long-term precision of our results is assessed by repeated analyses of pure "in-house" Li standard solutions (UMD-1 and IRMM-016) performed over the course of our analyses. Our average δ^7Li results are +54.9 ± 0.5 (2σ, n=8) for UMD-1, and +0.4 ± 0.5 (2σ, n=8) for IRMM-016 (Supplementary File A and Supplementary Table C). Given our long-term reproducibility, the 2 sigma analytical uncertainty adopted in this study for the Li isotopic composition is ±1‰.

4. Results

New major element concentrations for the Tajikistan loesses and previously published data for all other samples are provided in Supplementary Table A. The reader is referred to the studies of Gallet et al. (1998; 1996) and Jahn et al. (2001) for a full description of major element concentrations in loess samples. Here, we briefly compare loess deposits as a function of their formation mechanism (i.e., periglacial vs. desert loesses) and as a function of their sampling locations. The first noticeable difference is that periglacial samples have higher SiO_2 concentrations (average of 76 ± 9 (2σ) wt% vs. 57 ± 12 (2σ) wt% for desert loesses) and lower contents of all the other major elements compared to the desert loesses (see Supplementary Table A). Among desert loesses, samples from Tajikistan, China, and Argentina form three distinct groups. Loesses from Tajikistan are generally more concentrated in Fe_2O_3, CaO, Al_2O_3, MnO and MgO than Chinese loesses, which are themselves more enriched in these elements than Argentinian loesses. The only exception is the high Al_2O_3 contents of the Argentinian loesses (See Supplementary Table A). By contrast, loesses from Tajikistan are, on average, depleted in SiO_2, K_2O and Na_2O compared to Chinese loesses, which are themselves lower than the Argentian loesses. Some of these features are illustrated in Figure 1 where we plot Al_2O_3/Na_2O vs. Fe_2O_3/SiO_2 showing that desert loesses follow a well-defined linear trend

whereas periglacial loesses scatter, in part due to their low Fe_2O_3 and high SiO_2 contents that translates into low Fe_2O_3/SiO_2 ratios. Among desert loesses, Tajikistan samples have higher Al_2O_3/Na_2O and Fe_2O_3/SiO_2 ratios than Chinese samples while Argentinian samples are somewhat lower but more variable.

Lithium concentrations and isotopic compositions are reported in Table 1 for all loesses and are plotted in Figures 2 and 3, respectively. As for major element concentrations, periglacial loesses differ from desert loesses in their Li compositions. Periglacial deposits show a wide range of δ^7Li values, between -2.9 and +4.7, with an average value of +0.1 ± 5.6 (2σ) (Fig. 3). This variability is also seen in the Li concentrations, which range from 17 to 61 ppm, with an average of 40 ± 39 (2σ) ppm (Fig. 2). Such variability is comparable to that seen in periglacial loess deposits investigated by Teng et al. (2004) from New Zealand, Germany, and the midwestern USA (δ^7Li : -3.1 to +4.8 ; [Li]: 17 to 41 ppm). Desert loesses have less variable Li concentrations and isotopic compositions (on average 37 ± 13 (2σ) ppm and +0.9 ± 3.0 (2σ) respectively; Fig. 2 and Fig. 3) and each locality also has distinct averages: the Tajiskistan samples have the highest [Li] and the lowest δ^7Li values ([Li]= 41 ± 15 (2σ) ppm and δ^7Li= -0.3 ± 1.2 (2σ); Fig. 3), the Chinese samples are intermediate ([Li]= 37 ± 6 (2σ) ppm and δ^7Li= +1.0 ± 2.0 (2σ); Fig. 3) while the Argentinian samples show the lowest [Li] but the heaviest Li isotopic composition ([Li]= 30 ± 9 (2σ) ppm and δ^7Li= +2.7 ± 3.5 (2σ); Fig. 3).

5. Discussion

5.1. Use of desert loess deposits to establish the Li isotopic composition of the upper continental crust (UCC)

Several studies have previously used loess deposits to estimate the average composition of the UCC (Taylor et al., 1983; Gallet et al., 1996; 1998; McLennan, 2001; Peucker Ehrenbrink and Jahn, 2001; Chauvel et al., 2014). Most of these studies focused on periglacial loesses. However, as can be seen in Figures 1 to 3, the two types of loess do not carry the same

183 information. Periglacial loess deposits appear to be enriched in quartz (as seen in their high SiO_2
184 and low Fe_2O_3/SiO_2, Fig. 1) and have a large range of Li concentrations and Li isotopic
185 compositions (Fig. 2 and 3), while desert loess are more homogeneous. Such variability can
186 result either from the presence of metamorphic and igneous rocks fragments derived from the
187 source (Swineford and Frye, 1955; Garçon et al., 2014); a "nugget effect" i.e. the over-
188 concentration of heavy minerals associated to quartz grains or reflect the preservation of
189 inherited isotopic variability from the source rocks due to short transport distances (Rousseau et
190 al., 2014).
191 Although heavy minerals, mainly zircons, have been shown to significantly influence
192 neodymium, hafnium and lead isotopic compositions of fine-grained sediments, including
193 loesses (Garçon et al., 2014, Chauvel et al., 2014), such effects are unlikely to be responsible
194 for the Li isotope variability we observe. Indeed, periglacial loesses are enriched in heavy
195 minerals such as zircons (Chauvel et al., 2014; Taylor et al., 1983; Taylor and McLennan, 1985),
196 as reflected by their very low Nd/Hf ratio (Fig. 3a), which is, on average, lower than 3.5 (Chauvel
197 et al., 2014). Zircons control the Hf but not the Nd budget of sediments (Garçon et al., 2014),
198 therefore, an excess of zircon in the sediments generates a low Nd/Hf ratio. Although zircons
199 have variable Li contents (0.5 to 250 ppm) and Li isotopic compositions, ranging from -24 to +14
200 (Bouvier et al., 2012; Ushikubo et al., 2008), characteristics that could explain some of the Li
201 variations seen in periglacial loesses, a mass balance calculation demonstrates that
202 heterogeneous distribution of zircon cannot be the cause of the Li isotopic variability. Here we
203 consider two extreme cases for Li in zircon ([Li]=250ppm; δ^7Li=-24 and [Li]=250ppm; δ^7Li=+14)
204 and we calculate that the presence of ≤ 0.5% zircon by mass (the average proportion of zircons
205 in periglacial loesses as suggested by Bronger (2003) and Rousseau et al. (2007)) can shift the
206 Li isotopic composition by no more than 1‰. Therefore, the Li variations in periglacial loesses
207 cannot be explained simply by an excess of zircons and a similar conclusion can probably be
208 drawn for the other heavy minerals (e.g. epidote, goethite and hematite).

Thus, preservation of Li isotopic variability inherited form the source is likely responsible for the Li heterogeneity observed in periglacial loesses. Such results are consistent with the conclusions of Chauvel et al. (2014) who focused on trace elements and Nd-Hf isotopic characteristics of loess and concluded that periglacial loess samples, in addition to being extremely variable regarding their trace element patterns, are likely too heterogeneous to be useful in deriving upper crustal averages for Nd and Hf. We conclude that the same is likely true for determining the average Li composition of the UCC. By contrast, desert loesses are transported over greater distances (Ding et al., 1999), are less enriched in heavy minerals such as zircons (mostly Nd/Hf > 3.5, Chauvel et al., 2014; , Fig. 3), and are well homogenized. As a consequence, their chemical composition is less biased, and they are better proxies for constraining the average composition of the UCC. We will thus only focus on the composition of the desert loesses in the following discussion.

5.2. Eolian mineralogical sorting controls Li within desert loess

It is essential to understand which processes control the variations of Li concentrations and isotopic compositions observed in the desert loess deposits and why each locality has a different average δ^7Li (Fig. 3). Because Li is a soluble element (Brenan et al., 1998) it is affected by weathering processes and Li concentration may vary due to post-depositional alteration. However, in desert loesses, positive correlations between Li contents and immobile elements such as the rare earth elements (REE) (Fig. 4) suggest that Li has not been significantly remobilized by post-depositional chemical weathering, which we refer to as present-day weathering, i.e., transformation into soils (Dellinger et al., 2014).

Another process that can lead to Li isotopic variability is source rock heterogeneity within the provenance (Dellinger et al., 2014, Qiu et al., 2009), i.e., mafic versus felsic or juvenile versus old crustal material. Based on the observation that Argentinian loesses are enriched in clasts of volcanic rocks (andesites, basalts, dacites, rhyolites) (Imbellone and Teruggi, 1993; Teruggi,

1957) and that young volcanogenic sediments tend to have higher δ^7Li (Bouman et al., 2004), one could link the observed variations in δ^7Li in desert loesses to the provenance of the dust. This assumption can be evaluated using source proxies that are not significantly affected by sedimentary processes, such as the ratio of insoluble elements Th/La (Plank, 2005) that traces the contribution of felsic and mafic materials, or the Nd isotopic composition (Goldstein et al., 1984) that is controlled by the proportion of young to old mantle-derived igneous rocks in the source region. If we consider the less evolved volcanic rocks (i.e., basalts) that should create the largest variability, we can see that the average Th/La ratio of desert loess samples of 0.37±0.04 (2σ), including the Argentinian samples, is similar to that of the UCC (~0.34 after Rudnick and Gao, 2014) but significantly different from the range known for Andean arc basalts (Fig. 5a). This suggests that the presence of mafic components in the provenance, such as Andean basalts in the Argentinian loess samples, is probably minimal and has had no effect on the Li isotopic compositions, as shown by the absence of correlation between Th/La and δ^7Li (Fig. 5a). Even though the Argentinian loesses tend to have higher ε_{Nd} (~ -2), which is explained by the presence of juvenile material in their source (Chauvel et al., 2014; Gallet et al., 1998; Smith et al., 2003), the lack of correlation between the Nd and the Li isotopic compositions of our samples (Fig. 5b) suggests that the Li isotopic compositions and concentrations of desert loesses are not mainly controlled by source heterogeneity.

When sediments are transported by wind, the finest and lightest particles are preferentially transported over longer distances compared to coarse and dense particles that accumulate close to the source regions (Pye, 1995). This is manifest as differences in the average grain size (Yang and Ding, 2004), mineralogy (Eden et al., 1994; Yang et al., 2006), and chemical composition (Feng et al., 2009; 2010; 2011) as a function of distance from their source regions. This grain-size dependence of the chemical composition has also been observed in other types of sediments (Bouchez et al., 2011; Carpentier et al., 2014; Dellinger et al., 2014; Garçon et al., 2014; 2013; Garzanti et al., 2011). Indeed, as minerals have different chemical and isotopic

compositions (Garçon et al., 2014; 2013; 2011), sediments with different grain-sizes, composed of different minerals in different proportions, will have different chemical compositions. For example, quartz is preferentially enriched in coarse-grained fractions (Garzanti et al., 2011; 2010), has very high δ^7Li of ~ +30 due to preferential enrichment of ^{7}Li in the 2- or 4-fold sites in quartz (Dennen et al., 1966; Maloney et al., 2008; Teng et al., 2006) and has relatively low [Li] of ~10 ppm (Dennen, 1966; Garçon et al., 2014; Lynton et al., 2005; Monecke et al., 2000; Teng et al., 2006). By contrast, clay minerals are enriched in the finest fractions (Garzanti et al., 2011; 2010) and have low δ^7Li of ~ -1 and high [Li] of ~63 ppm (Qiu et al., 2009; Romer et al., 2014; Tsai et al., 2014). Consequently, one could expect fine-grained sediments, preferentially enriched in clays, to have higher Li concentrations and lower δ^7Li than coarse-grained sediments that are preferentially enriched in quartz.

In desert loesses, the well-defined correlations between both [Li] and REE (Fig.4), δ^7Li and Nd/Hf (Fig. 3a), δ^7Li and Fe_2O_3/SiO_2 (Fig. 3b), as well as between Al_2O_3/Na_2O and Fe_2O_3/SiO_2 (Fig. 1), suggest that the bulk composition and most Li variations are related to the sediment grain-size. Indeed, Fe_2O_3, Al_2O_3 and REE are preferentially enriched in the fine-grained fraction of the loesses because phyllosilicates (clays and micas) are rich in iron, aluminium and REE (Garçon et al., 2014; Taylor and McLennan, 1985). By contrast, Na_2O, SiO_2 and Hf are mostly hosted in plagioclase, quartz and zircons, respectively, three mineral phases that are abundant in the coarse fraction (Eden et al., 1994; Garzanti et al., 2011; Yang et al., 2006). As a consequence, Nd/Hf, Al_2O_3/Na_2O and Fe_2O_3/SiO_2 ratios are excellent proxies for grain-sizes and reflect transport-driven compositional changes. This observation is consistent with the average grain-size of the samples as determined by previous studies. The Tajikistan samples are the finest loess samples (6 to 12 µm, Ding and Ding, 2003; Fig. 1) and have the highest [Li] and the lowest δ^7Li values, while the Argentinian samples are the coarsest samples (>40 µm, Teruggi, 1957; Fig.1) and have the lowest [Li] and the highest δ^7Li values.

The major minerals of desert loesses: quartz, plagioclase and phyllosilicates (Eden et al., 1994;

Gallet et al., 1996; Jeong et al., 2008; 2011), can be mixed to produce the observed range of Li compositions (Fig. 6). Both Li concentrations and Li isotopic compositions are controlled by mineral sorting between a fine-grained end-member, enriched in phyllosilicates (clays and micas) - with a high [Li] and a low δ^7Li - and a coarse-grained end-member, enriched in quartz and plagioclase - with a low [Li] and a high δ^7Li (see caption of Figure 6 for more details). Isotopic mixing calculations allow us to quantify the amount of unweathered, coarse-grained vs. weathered, fine-grained particles (Fig. 6). The results of the mixing calculations match the modal mineralogical proportions estimated from previous studies of the Chinese and Argentinian loess deposits (Camilión, 1993; Jeong et al., 2011; 2008; Teruggi, 1957) (Fig. 6). For example, the relative average proportions of phyllosilicates, quartz, and plagioclase given by our mixing calculations for the Argentinian loess are 40 wt.%, 36 wt.%, and 24 wt.% respectively, while the average modal proportions reported by Camilion (1993) and Teruggi (1957) are 40 wt.%, 33 wt.%, and 27 wt.% respectively. There are no estimated mineral proportions for the Tajikistan samples. Nevertheless, their average grain-size is smaller than the other loess deposits (<12 μm, Ding and Ding, 2003), which is consistent with the higher phyllosilicate proportion estimated from our isotopic mixing calculations (Fig. 6). Significant contributions from mafic minerals such as amphibole, which can contain appreciable Li (Marks et al., 2008), can be ruled out. Indeed, if we assume that our Li variations are partly controlled by mafic minerals (mainly amphibole), we cannot reproduce the Li variations observed in the desert loess deposits. Moreover, because the abundance of mafic minerals in desert loess samples is very low (proportions < 4 wt.%, (Eden et al., 1994; Jeong et al., 2008; Teruggi, 1957) relative to quartz, plagioclase and phyllosilicates, they cannot control the Li variations. Based on these observations, we conclude that the variations of δ^7Li and [Li] in desert loesses can be understood in terms of relatively simple mixing between minerals of different grain size fractions, as shown in Fig. 6.

5.3. A new estimate of the δ^7Li and [Li] in the average upper continental crust

313 Estimating the composition of the average UCC using sediments dates back to the work of
314 Goldschmidt in the 1930's. This can be done either using an average composition of sediments,
315 assuming that no processes had biased their composition compared to their source rocks, or
316 using correlations observed in the concentrations of insoluble elements (McLennan, 2001).
317 Because of the mineralogical sorting observed in our desert loess samples, it is not advisable to
318 use their average composition as a representative value for the UCC and we focus here on the
319 second method.
320 Figure 4 shows well-defined correlations observed for desert loesses between Li and immobile
321 elements, in this case, the REE. As REE are preferentially enriched in fine-grained sediments
322 (Garçon et al., 2014; Taylor and McLennan, 1985), such trends reflect mixing lines between a
323 fine-grained end-member (enriched in REE and Li) and a coarse-grained end-member (depleted
324 in REE and Li). Using the correlations between Li and REE that are assumed to have the same
325 behavior as Li during magmatic differentiation (i.e., Sm to Er) (Ryan and Langmuir, 1987), we
326 estimate a new average Li concentration for the UCC (Fig. 4). For each of the seven correlations
327 (i.e., Li vs. Sm, Li vs. Eu, Li vs. Gd, Li vs. Tb, Li vs. Dy, Li vs. Ho and Li vs. Er; Fig. 4), we start
328 with the raw data and first run a Monte-Carlo routine to estimate the uncertainties on the slopes
329 and intercepts of the linear regressions. For each individual data point, we thus randomly sample
330 a value within the uncertainty of the measured data point to generate a synthetic dataset. We
331 then fit a straight line through all of the synthetic datasets using weighted linear regressions
332 following the algorithm of York et al. (2004) that has been implemented in MATLAB^{TM} by
333 Thirumalai et al. (2011). Within this first Monte-Carlo routine, we perform a second Monte-Carlo
334 simulation to interpolate [Li] at the REE concentrations published by Rudnick and Gao (2014) for
335 the UCC, taking into account the uncertainties on the REE concentrations published by Rudnick
336 and Gao (2014) (see supplementary file B for more details). We then compile all the interpolated
337 [Li] and calculate both the average and the standard deviation of the distribution. Using this
338 method, we obtain an average Li concentration of 30.5 ± 3.6 (2σ) ppm for the UCC, in

agreement with the previously published values of Teng et al. (2004; 35 ± 11 (2σ) ppm) and Rudnick and Gao (2014; 24 ± 10 ppm) but with a significantly lower uncertainty. Our value is somewhat lower than the derived by Hu and Gao (41 ± 6 (2σ) ppm) on the basis of correlations between Li and In observed in various sediments and sedimentary rocks.

Following the same procedure (weighed linear regression followed by interpolation using Monte-Carlo simulations), we estimate the average δ^7Li of the UCC using the correlations between δ^7Li and two independent ratios of immobile elements that are not significantly affected by chemical weathering processes, namely, Nd/Hf (Fig. 3a) and Fe_2O_3/SiO_2 (Fig. 3b). These two ratios are good grain-size proxies (see previous section) and are relatively well known in the UCC (Nd/Hf = 5.1 ± 2.1 (2σ) and Fe_2O_3/SiO_2= 0.084 ± 0.02 (2σ), Rudnick and Gao, 2014). Interpolating these values on the regression lines, we get two sets of values having consistent average Li isotopic compositions: δ^7Li = +0.8 ± 0.4 (2σ) using the correlation between δ^7Li and Nd/Hf (Fig.3a) and δ^7Li = +0.4 ± 0.4 (2σ) using the correlation between δ^7Li and Fe_2O_3/SiO_2 (Fig.3b). Combining these two sets of data, we obtain an average δ^7Li = +0.6 ± 0.6 (2σ) (see supplementary file B for more explanations). Here again, this new estimate is within the uncertainties of the previously published value of 0 ± 4 (2σ) (Teng et al., 2004), but with a much smaller uncertainty.

5.4. Determining the average weathering signature of upper continental crust

Chemical weathering is an important process affecting the composition of the continental crust (Dellinger et al., 2014) because it involves the breakdown of rocks into secondary phases such as clays and hydroxides, and it releases soluble elements to the hydrosphere. It has been suggested that this process progressively modifies the chemical composition of the Earth's surface (Albarede, 1998; Lee et al., 2008; Liu and Rudnick, 2011; Rudnick, 1995) but the degree of weathering experienced in the past within the average UCC and quantified by the proportion of weathered sedimentary rocks exposed at the Earth's surface is still poorly known.

Silicate rock weathering is very important in the worldwide atmospheric CO_2 consumption occurring today (Amiotte Suchet et al., 2003; Dessert et al., 2003; Gaillardet et al., 1999; Jin et al., 2014). Hence, through the disintegration of pre-existing rocks, chemical weathering acts as sink for atmospheric CO_2, and so indirectly controls the evolution of our climate. Shales appear to have a significant influence on global CO_2 consumption, accounting for 40% of the total CO_2 consumed worldwide (Amiotte Suchet et al., 2003), but only a few studies have tried to quantify their abundances on continents and these studies show rather large discrepancies. Blatt and Jones (1975) estimate that 66% of the rocks exposed on the Earth's surface are sedimentary rocks, but estimates for the proportion of shales are less well known and differ widely between 13 and 34% (Amiotte Suchet et al., 2003; Condie, 1993; Gibbs and Klump, 1994; Meybeck, 1987). An isotopic approach could potentially provide a more robust estimate of the average degree of weathering experienced by the UCC, and help us to understand the processes controlling the compositional evolution of the upper crust.

Figure 7 shows how δ^7Li varies as a function of CIA (Chemical Index of Alteration) in the loess deposits. The CIA, calculated as the ratio of major elements (Al_2O_3 /[Al_2O_3 +CaO*+Na_2O+K_2O], see caption of Fig. 7 for more details), measures the loss of mobile cations (Ca^{2+}, K^+ and Na^+) present in labile minerals (feldspars, pyroxenes, amphiboles) relative to the amount of Al^{3+} that is preserved in more stable minerals (i.e., clay) under surface conditions (Nesbitt and Young, 1982). Hence, the CIA is a good proxy for the intensity of chemical weathering: the higher the CIA, the greater the degree of weathering the sample has experienced in the past. In Figure 7, we show that the range of δ^7Li and CIA values obtained for the desert loess deposits follow a binary isotopic mixing trend between unweathered, mantle-derived igneous rocks (i.e., I-type granites) with high δ^7Li and low CIA, and a weathered component (i.e., shales) with low δ^7Li and high CIA. The Li composition (δ^7Li= -0.9 ± 4.7 (2σ) ; [Li] = 66 ± 92 (2σ) ppm) and CIA value (CIA= 74 ± 21 (2σ)) of the weathered end-member (shale) is compiled from several studies (Hu and Gao, 2008; Moriguti and Nakamura, 1998b; Qiu et al., 2009; Romer et al., 2014; Tang et al.,

2014; Teng et al., 2004, and unpublished data of Su Li and others), while values for the unweathered end-member (Clarence River Supersuite I-type granite) come from Bryant et al. (2004) (δ^7Li = +4.3 ± 4.1 (2σ), [Li]= 17 ± 18 (2σ) ppm and CIA= 54 ± 8 (2σ)). These granites differentiated from mantle-derived magma and have not incorporated any meta-sedimentary materials (Bryant et al., 2004), which is important as the unweathered end-member should not include weathered materials, which many other I-type granites do (Teng et al., 2004). Unfortunately, the compositions of the two end-members are not very well constrained (large uncertainties on the averages) and the large errors can have a non-negligible impact on our isotopic mixing calculation. However, the very good consistency observed between the isotopic modeling and our data suggests these average values of the two end-members are realistic.

The UCC is considered to have a granodioritic composition (Arndt, 2013; Eade and Fahrig, 1973; Rudnick and Gao, 2014; Taylor and McLennan, 1985) and juvenile crust should have the high δ^7Li and low CIA values shown in Figure 7 for igneous rocks that are devoid of a sedimentary component in their source regions. As its composition is modified by chemical weathering, the Li isotopic composition of the UCC decreases, with a concomitant increase of its CIA, reaching, in extreme cases, the very low δ^7Li and high CIA values found in shales (Fig. 7). It is therefore reasonable to expect that the present-day UCC falls on a mixing line between an unweathered component (granites) and a weathered one (shales). Using our estimate for the average δ^7Li of upper crust and the results of the isotopic mixing, we derive the average CIA of present-day UCC to be between 59 and 65 with an average of 61 (Fig. 7). This new value differs from the average value given by Rudnick and Gao (2014) for the upper crust (CIA = 53, calculated using the average major element concentrations), and which is derived from a compilation of several studies, mainly based on sampling widespread outcrop exposures. This discrepancy may reflect inadequate sampling methods, as a majority of these studies focused on a limited part of the world (e.g., North Craton China (Gao et al., 1998) and Canadian Precambrian shield (Eade and Fahrig, 1973; Shaw et al., 1976; 1967)). The low CIA may thus

reflect local composition where the proportion of weathered rocks is lower than the average UCC. Or, as these studies rely only on outcrops at the Earth's surface, the discrepancy can be explained by the presence of under-sampled sedimentary rocks that occur in fold belts and continental platforms, as previously suggested by Amiotte-Suchet et al. (2003).

Our new CIA estimate is also significantly lower than the value estimated for Archean UCC (average CIA = 77) and for Paleoproterozoic UCC (average CIA = 67) as determined by Gaschnig et al. (2014) using ancient glacial diamictites. The higher CIA in the past has been interpreted as resulting from more intense weathering (Gaschnig et al., 2014). Condie (1993) reached a similar conclusion on the basis of the depletion in Na, Ca and Sr in Archean shales, which he suggested reflected more intense chemical weathering during the Archean. Therefore, the difference between the present-day and ancient CIA of the UCC may reflect a change in the intensity of chemical weathering through time that modified the chemical composition of the UCC.

Another approach to quantify the importance of past chemical weathering is to determine the amount of weathered products produced by this process. Our novel isotopic approach shows that the chemical composition of the present upper continental crust, having a δ^7Li of +0.6±0.6 and a CIA of 61, can be explained by a mixture of 63^{+10}_{-17} (2σ) % of unweathered igneous rocks (granites) and 37^{+17}_{-10} (2σ) % of rocks produced by weathering (shales) (cf. Fig. 7). The inferred proportion of shales is slightly higher than previous estimates. Amiotte-Suchet et al. (2003) have shown that ~25% shales present at the Earth's surface accounts for about 40% of the CO_2 drawdown in the atmosphere. With ~40% shales at the surface, as estimated here, almost 60% of the worldwide CO_2 could be consumed, highlighting how important weathering may be for the overall CO_2 budget of the Earth. This deserves more attention, particularly from a climate studies point of view. Thus, both means of estimating the average weathering signature of the UCC (average CIA and mixing of shales and granites) demonstrate that weathering has had a profound influence on the average composition of the UCC and, based on the relationship

between weathering and CO_2 draw-down, the continental crust has, in turn, profoundly influenced climate.

6. Summary and conclusions

Based on analyses of global loess samples, periglacial loesses are too heterogeneous to be used as proxies to estimate the Li composition of the upper continental crust. Desert loess deposits appear to be more homogenous and thus more suitable to infer average Li values. The Li isotopic compositions and concentrations of desert loesses are controlled by mineralogical sorting and can be reproduced by mixing between a fine-grained, weathered end-member (i.e., phyllosilicates) and a coarse-grained, relatively unweathered end-member (i.e., a mixture of quartz and plagioclase). Using the correlations between Li and REE concentrations in the desert loesses we derive a new estimate for the average Li concentration of the upper crust: 30.5 ± 3.6 (2σ) ppm. Similarly, using correlations between δ^7Li and independent ratios of immobile elements, we estimate an average δ^7Li= +0.6 ± 0.6 (2σ) for the UCC. These results are similar to previous estimates, but are more precisely constrained, and show that the UCC carries a significantly more weathered signature than fresh mantle-derived rocks. Using an isotopic mixing approach we also quantify the cumulative importance of chemical weathering on the continents over Earth history. We estimate that 37^{+17}_{-10} (2σ) % of the current upper crust is composed of highly weathered sediments (i.e., shales) that are the by-products of chemical weathering experienced in the past and that the UCC's present CIA is 61^{+4}_{-2}, 2σ, which is lower than what it was in the Paleoproterozoic and Archean periods, but higher than previous estimates of the UCC. Our results thus provide a framework from which to compare the UCC through time.

Acknowledgments

We thank S. Gallet and B.M. Jahn for providing the samples analyzed in this study. We also greatly thank S. Bureau for major element analyses, I.S. Puchtel for his help in the clean

laboratory, as well as R.D. Ash for his assistance during isotopic measurements. Thanks also to X.-M. Liu and W.F. McDonough for constructive discussions and advices that helped improve the content of the manuscript. We thank reviewers Mathieu Dellinger and Edward Tipper for their comments that helped improve the manuscript and editor Mike Bickle for his pleasant comments and efficient editorial handling. This work was supported by NSF grant EAR 0948549 and INSU-CNRS, the University of Grenoble as well as Rhône-Alpes region.

Table Captions

Table 1: Li isotopic compositions and concentrations of loess samples

** $\delta^7Li = [(^7Li/^6Li)_{sample}/(^7Li/^6Li)_{L\text{-}SVEC} - 1)*1000$ in ‰. L-SVEC data comes from Flesch et al. (1973).*

*** Li concentrations are from Chauvel et al. (2014). "dup" stands for complete duplicate analysis*

Figure Captions

Figure 1: Plot of grain-size proxies (Al_2O_3/Na_2O vs. Fe_2O_3/SiO_2) illustrating the differences between periglacial and desert loess samples.

Periglacial loesses include data from this study, as well as literature data (light blue) from Teng et al. (2004)*. Fine-grained particles such as clays have high Al_2O_3/Na_2O and Fe_2O_3/SiO_2. Desert loesses plot on a well-defined mixing array, whereas periglacial loesses show greater scatter. Data for the Chinese loess come from Gallet et al.* (1996) *and Jahn et al.* (2001) *and from Gallet et al.* (1998) *for the Argentinian and Western Europe loess. The correlation coefficients R^2 are calculated for desert loesses only. Error bars represent 2σ.*

Figure 2: Stacked histogram of [Li] in desert (red) and periglacial (blue) loess deposits.

Periglacial loesses include data from this study, as well as data from Teng et al. (2004)*. Li concentrations for the samples analyzed in this study are from Chauvel et al.* (2014)*.*

Figure 3: Variations of a) δ^7Li versus Nd/Hf and b) δ^7Li versus Fe_2O_3/SiO_2 for all loess samples Dark blue data points are periglacial loess deposits from Western Europe analyzed in this study. Literature data (light blue) are from Teng et al. (2004) for periglacial loess deposits from New Zealand, Germany and the midwestern USA. Nd and Hf concentrations of desert loesses are from Chauvel et al. (2014). As Hf and SiO_2 are enriched in zircon and quartz respectively, the correlations observed for desert loesses reflect mixing between two grain-size end-members. The average Nd/Hf and Fe_2O_3/SiO_2 values for the upper continental crust are 5.1 ± 2.1 (2σ) and 0.084 ± 0.02 (2σ) respectively (Rudnick and Gao (2014)*). For each correlation, the average δ^7Li of the UCC, together with its uncertainty, have been estimated using a weighted linear regression (York et al.,* (2004) *to fit a straight line through the data, followed by a Monte-Carlo simulation to interpolate δ^7Li, taking into account the errors on the slopes and intercepts of the regression lines, as well as the uncertainties on the average Nd/Hf and Fe_2O_3/SiO_2 ratios of the UCC published by Rudnick and Gao (2014) (see supplementary file B for more details). Gray field represents uncertainties on the linear regressions derived from Monte Carlo simulations. Error bars represent 2σ.*

Figure 4: [Li] versus rare earth elements (REE) in desert loess samples.
For each correlation we used a weighted linear regression (York et al., (2004) *followed by a Monte-Carlo simulation to interpolate [Li] and its uncertainty at the average REE concentration of the UCC published by Rudnick and Gao (2014). By averaging all of these values, we infer the average [Li] of the UCC (see supplementary file B for more details). Gray field represents uncertainties on the linear regressions derived from Monte Carlo simulations. Errors bars represent 2σ uncertainty.*

Figure 5: a) δ^7Li versus Th/La and b) δ^7Li versus ε_{Nd} in desert loess samples.

The range of Th/La ratio for the UCC is from Rudnick and Gao (2014) *(excluding data from Eade and Fahrig (1973) due to XRF-determined La leading to anomalously high values). The average* ε_{Nd} *for the UCC is from Chauvel et al. (2014). Arrays represent the range of estimates for the UCC (gray) given by Rudnick and Gao* (2014) *for Th/La and by Chauvel et al.* (2014) *for* ε_{Nd}*. Data for Andean basalts (green) are from the GEOROC database. Error bars are 2σ.*

Figure 6: Isotopic mixing between a fine-grained end-member enriched in phyllosilicates (Ph) and a coarse-grained end-member composed of a mixture of quartz (Qtz) and plagioclase (Pl). All the end-member values come from the literature. For phyllosilicates (mica, chlorite and clay minerals): [Li] ≈ 63 ppm and $\delta^7Li \approx -1$ (Bouman et al., 2004; Garçon et al., 2014; Tsai et al., 2014)*, for quartz: [Li] ≈ 10 ppm and* $\delta^7Li \approx +30$ (Dennen, 1966; Garçon et al., 2014; Lynton et al., 2005; Monecke et al., 2000; Teng et al., 2006) *and for plagioclase : [Li] ≈ 2 ppm and* $\delta^7Li \approx +2.5$ *(*δ^7Li *values from equilibrated plagioclase only;* (Bindeman and Bailey, 1999; Bindeman et al., 1999; Cabato et al., 2013; Teng et al., 2008)*. Equations used for isotopic mixing are from Langmuir et al.* (1978)*. Ticks on the mixing lines correspond to 10% increments in the proportions of phyllosilicates, quartz and plagioclase. Analytical errors are 2σ.*

Figure 7: δ^7Li *versus CIA (Chemical Index of Alteration) in desert loess samples. CIA is the molar ratio* $Al_2O_3/(Al_2O_3 + CaO^* + Na_2O + K_2O)$*, where CaO* refers to Ca contained in silicates* (McLennan et al., 1993; Nesbitt and Young, 1982)*. A correction is done to consider the presence of carbonates (calcite and dolomite) and phosphates (apatite). Correction for Ca in apatite is based on* P_2O_5 *concentration, while correction for Ca in carbonate is generally done on the basis of* CO_2 *concentrations. When such data are not available, reasonable* CaO/Na_2O *ratios in silicate can be assumed (i.e.* $CaO/Na_2O < 1$*) following the argument of McLennan* (1993)*. CIA for the loess samples from China, and Argentina were calculated using the major element data of Gallet et al.* (1996)*, Jahn et al.* (2001) *and Gallet et al.* (1998)*. The black dotted line shows the*

binary mixing model between the highly weathered end-member (i.e., shales, blue star) and the unweathered igneous rocks (i.e., I-type granites without meta-sedimentary component in the source, green star). The equations used for the isotopic mixing are from Langmuir et al. (1978)*. Diamonds on the mixing line correspond to 10% increments in the proportion of weathered component. The pale red field represents 2σ uncertainty on the interpolated CIA*.

References

Albarede, F., 1998. The growth of continental crust. Tectonophysics 296, 1–14.

Amiotte Suchet, P., Probst, J.-L., Ludwig, W., 2003. Worldwide distribution of continental rock lithology: Implications for the atmospheric/soil CO2 uptake by continental weathering and alkalinity river transport to the oceans. Global Biogeochemical Cycles 17. doi:10.1029/2002GB001891

Arndt, N.T., 2013. Formation and Evolution of the Continental Crust. Geochemical perspectives. doi:10.7185/geochempersp.2.3

Bindeman, I.N., Bailey, J.C., 1999. Trace elements in anorthite megacrysts from the Kurile Island Arc:a window to across-arc geochemical variations in magma compositions. Earth and Planetary Science Letters 1–18.

Bindeman, I.N., Davis, A.M., Wickham, S.M., 1999. 400 my of basic magmatism in a single lithospheric block during cratonization: Ion microprobe study of plagioclase megacrysts in mafic rocks from Transbaikalia, Russia. Journal of Petrology 40, 807–830.

Blatt, H., Jones, R.L., 1975. Proportions of exposed igneous, metamorphic, and sedimentary rocks. Geology 86, 1085–1088.

Bouman, C., Elliott, T., Vroon, P.Z., 2004. Lithium inputs to subduction zones. Chemical Geology 212, 59–79. doi:10.1016/j.chemgeo.2004.08.004

Bouchez, J., Gaillardet, J., France-Lanord, C., Maurice, L., Dutra-Maia, P., 2011. Grain size control of river suspended sediment geochemistry: clues from Amazon River depth profiles. Geochem. Geophys. Geosyst.12, Q03008.

Bouvier, A.-S., Ushikubo, T., Kita, N.T., Cavosie, A.J., Kozdon, R., Valley, J.W., 2012. Li isotopes and trace elements as a petrogenetic tracer in zircon: insights from Archean TTGs and sanukitoids. Contrib Mineral Petrol 163, 745–768. doi:10.1007/s00410-011-0697-1

Brenan, J.M., Ryerson, F.J., Shaw, H.F., 1998. The role of aqueous fluids in the slab-to-mantle transfer of boron, beryllium, and lithium during subduction: Experiments and models.

577 Geochemica and Cosmochimica Acta 62, 3337–3347.
578 Bronger, A., 2003. Correlation of loess–paleosol sequences in East and Central Asia with SE
579 Central Europe: towards a continental Quaternary pedostratigraphy and paleoclimatic
580 history. Quaternary International 106, 11–31.
581 Bronger, A., Heinkele, T., 1990. Mineralogical and clay mineralogical aspects of loess research.
582 Quaternary International 7, 37–51.
583 Bryant, C.J., Chappell, B.W., Bennett, V.C., McCulloch, M.T., 2004. Lithium isotopic
584 compositions of the New England Batholith: correlations with inferred source rock
585 compositions. Transactions of the Royal Society of Edinburgh; Earth Sciences Vol. 95, 199–
586 214.
587 Cabato, J., Altherr, R., Ludwig, T., Meyer, H.-P., 2013. Li, Be, B concentrations and δ7Li values
588 in plagioclase phenocrysts of dacites from Nea Kameni (Santorini, Greece). Contrib Mineral
589 Petrol 165, 1135–1154. doi:10.1007/s00410-013-0851-z
590 Camilión, M.C., 1993. Clay mineral composition of Pampean loess (Argentina). Quaternary
591 International 17, 27–31.
592 Carpentier, M., Weis, D., Chauvel, C., 2014. Fractionation of Sr and Hf isotopes by mineral
593 sorting in Cascadia Basin terrigenous sediments. Chemical Geology 382, 67–82.
594 doi:10.1016/j.chemgeo.2014.05.028
595 Chan, L.-H., Edmond, J.M., Thompson, G., Gillis, K., 1992. Lithium Isotopic Composition of
596 Submarine Basalts - Implications for the Lithium Cycle in the Oceans. Earth and Planetary
597 Science Letters 108, 151–160.
598 Chauvel, C., Bureau, S., Poggi, C., 2011. Comprehensive Chemical and Isotopic Analyses of
599 Basalt and Sediment Reference Materials. Geostandards and Geoanalytical Research 35,
600 125–143. doi:10.1111/j.1751-908X.2010.00086.x
601 Chauvel, C., Garçon, M., Bureau, S., Besnault, A., Jahn, B.-M., Ding, Z., 2014. Constraints from
602 loess on the Hf–Nd isotopic composition of the upper continental crust. Earth and Planetary
603 Science Letters 388, 48–58. doi:10.1016/j.epsl.2013.11.045
604 Condie, K.C., 1993. Chemical composition and evolution of the upper continental crust:
605 contrasting results from surface samples and shales. Chemical Geology 104, 1–37.
606 Dellinger, M., Gaillardet, J., Bouchez, J., Calmels, D., Galy, V., Hilton, R.G., Louvat, P., France-
607 Lanord, C., 2014. Lithium isotopes in large rivers reveal the cannibalistic nature of modern
608 continental weathering and erosion. Earth and Planetary Science Letters 401, 359–372.
609 doi:10.1016/j.epsl.2014.05.061
610 Dennen, W.H., 1966. Stoichiometric Substitution in Natural Quartz. Geochimica et

611 Cosmochimica Acta 30, 1235–&. doi:10.1016/0016-7037(66)90122-0
612 Dessert, C., Dupré, B., Gaillardet, J., François, L.M., Allègre, C.J., 2003. Basalt weathering laws
613 and the impact of basalt weathering on the global carbon cycle. Chemical Geology 202,
614 257–273. doi:10.1016/j.chemgeo.2002.10.001
615 Ding, F., Ding, Z., 2003. Chemical weathering history of the southern Tajikistan loess and
616 paleoclimate implications. Science in china series D-Earth sciences 46, 1012–1021.
617 doi:10.1360/03yd0344
618 Ding, Z., Sun, J., Rutter, N.W., Rokosh, D., Liu, T., 1999. Changes in sand content of loess
619 deposits along a north–south transect of the Chinese Loess Plateau and the implications for
620 desert variations. Quaternary Research 52, 56–62.
621 Ding, Z.L., Ranov, V., Yang, S.L., Finaev, A., Han, J.M., Wang, G.A., 2002. The loess record in
622 southern Tajikistan and correlation with Chinese loess. Earth and Planetary Science Letters
623 200, 387–400.
624 Eade, K.E., Fahrig, W.F., 1973. Regional, Lithological, and Temporal Variation in the
625 Abundances of Some Trace Elements in the Canadian Shield.
626 Eden, D.N., Qizhong, W., Hunt, J.L., Whitton, J.S., 1994. Mineralogical and geochemical trends
627 across the Loess Plateau, North China. Catena 21, 73–90.
628 Elliott, T., Thomas, A., Jeffcoate, A., Niu, Y., 2006. Lithium isotope evidence for subduction-
629 enriched mantle in the source of mid-ocean-ridge basalts. Nature 443, 565–568.
630 doi:10.1038/nature05144
631 Feng, J.-L., Hu, Z.-G., Ju, J.-T., Zhu, L.-P., 2011. Variations in trace element (including rare
632 earth element) concentrations with grain sizes in loess and their implications for tracing the
633 provenance of eolian deposits. Quaternary International 236, 116–126.
634 doi:10.1016/j.quaint.2010.04.024
635 Feng, J.-L., Zhu, L.-P., Zhen, X.-L., Hu, Z.-G., 2009. Grain size effect on Sr and Nd isotopic
636 compositions in eolian dust: implications for tracing dust provenance and Nd model age.
637 Geochem. J 43, 123–131.
638 Feng, J.L., Hu, Z.G., Cui, J.Y., Zhu, L.P., 2010. Distributions of lead isotopes with grain size in
639 aeolian deposits. Terra Nova no–no. doi:10.1111/j.1365-3121.2010.00941.x
640 Flesch, G.D., Anderson, A.R., Jr., Svec, H.J., 1973. A secondary isotopic standard for 6Li/7Li
641 determinations. International Journal of Mass Spectrometry and Ion Physics 12, 265–272.
642 doi:10.1016/0020-7381(73)80043-9
643 Gaillardet, J., Dupré, B., Louvat, P., Allegre, C.J., 1999. Global silicate weathering and CO2
644 consumption rates deduced from the chemistry of large rivers. Chemical Geology 159, 3–30.

Gallet, S., Jahn, B.-M., Torii, M., 1996. Geochemical characterization of the Luochuan loess-paleosol sequence, China, and paleoclimatic implications. Chemical Geology 133, 67–88.

Gallet, S., Jahn, B.-M., Van Vliet Lanoë, B., Dia, A., Rossello, E., 1998. Loess geochemistry and its implications for particle origin and composition of the upper continental crust. Earth and Planetary Science Letters 156, 157–172.

Gao, S., Luo, T.-C., Zhang, B.-R., Zhang, H.-F., Han, Y.-W., Zhao, Z.-D., Hu, Y.-K., 1998. Chemical composition of the continental crust as revealed by studies in East China. Geochimica et Cosmochimica Acta 62, 1959–1975.

Garçon, M., Chauvel, C., Bureau, S., 2011. Beach placer, a proxy for the average Nd and Hf isotopic composition of a continental area. Chemical Geology 287, 182–192. doi:10.1016/j.chemgeo.2011.06.007

Garçon, M., Chauvel, C., France-Lanord, C., Huyghe, P., Lavé, J., 2013. Continental sedimentary processes decouple Nd and Hf isotopes. Geochimica et Cosmochimica Acta 121, 177–195. doi:10.1016/j.gca.2013.07.027

Garçon, M., Chauvel, C., France-Lanord, C., Limonta, M., Garzanti, E., 2014. Which minerals control the Nd–Hf–Sr–Pb isotopic compositions of river sediments? Chemical Geology 364, 42–55. doi:10.1016/j.chemgeo.2013.11.018

Garzanti, E., Andò, S., France-Lanord, C., Censi, P., Pietro Vignola, Galy, V., Lupker, M., 2011. Mineralogical and chemical variability of fluvial sediments 2. Suspended-load silt (Ganga-Brahmaputra, Bangladesh). Earth and Planetary Science Letters 302, 107–120. doi:10.1016/j.epsl.2010.11.043

Garzanti, E., Andò, S., France-Lanord, C., Vezzoli, G., Censi, P., Galy, V., Najman, Y., 2010. Mineralogical and chemical variability of fluvial sediments 1. Bedload sand (Ganga-Brahmaputra, Bangladesh). Earth and Planetary Science Letters 299, 368–381. doi:10.1016/j.epsl.2010.09.017

Gaschnig, R.M., Rudnick, R.L., McDonough, W.F., Kaufman, A.J., Hu, Z., Gao, S., 2014. Onset of oxidative weathering of continents recorded in the geochemistry of ancient glacial diamictites. Earth and Planetary Science Letters 408, 87–99. doi:10.1016/j.epsl.2014.10.002

Gibbs, M.T., Klump, L.R., 1994. Global chemical erosion during the last glacial maximum and the present: Sensitivity to changes in lithology and hydrology. Paleoceanography vol.9, 529–543.

Goldstein, S.L., O'nions, R.K., Hamilton, P.J., 1984. A Sm-Nd isotopic study of atmospheric dusts and particulates from major river systems. Earth and Planetary Science Letters 70, 221–236.

679 Haase, D., Fink, J., Haase, G., Ruske, R., Pécsi, M., Richter, H., Altermann, M., Jäger, K.D.,
680 2007. Loess in Europe—its spatial distribution based on a European Loess Map, scale
681 1:2,500,000. Quaternary Science Reviews 26, 1301–1312.
682 doi:10.1016/j.quascirev.2007.02.003
683 Hu, Z., Gao, S., 2008. Upper crustal abundances of trace elements: A revision and update.
684 Chemical Geology 253, 205–221. doi:10.1016/j.chemgeo.2008.05.010
685 Imbellone, P.A., Teruggi, M.E., 1993. Paleosols in loess deposits of the Argentine Pampas.
686 Quaternary International 17, 49–55.
687 Jahn, B.-M., Gallet, S., Han, J., 2001. Geochemistry of the Xining, Xifeng and Jixian sections,
688 Loess Plateau of China: eolian dust provenance and paleosol evolution during the last 140
689 ka. Chemical Geology 178, 71–94.
690 Jeong, G.Y., Hillier, S., Kemp, R.A., 2008. Quantitative bulk and single-particle mineralogy of a
691 thick Chinese loess–paleosol section: implications for loess provenance and weathering.
692 Quaternary Science Reviews 27, 1271–1287. doi:10.1016/j.quascirev.2008.02.006
693 Jeong, G.Y., Hillier, S., Kemp, R.A., 2011. Changes in mineralogy of loess–paleosol sections
694 across the Chinese Loess Plateau. Quaternary Research 75, 245–255.
695 doi:10.1016/j.yqres.2010.09.001
696 Jin, L., Ogrinc, N., Yesavage, T., Hasenmueller, E.A., Ma, L., Sullivan, P.L., Kaye, J., Duffy, C.,
697 Brantley, S.L., 2014. The CO2 consumption potential during gray shale weathering: Insights
698 from the evolution of carbon isotopes in the Susquehanna Shale Hills critical zone
699 observatory. Geochimica et Cosmochimica Acta 142, 260–280.
700 doi:10.1016/j.gca.2014.07.006
701 Kısakürek, B., James, R.H., Harris, N.B.W., 2005. Li and δ7Li in Himalayan rivers: Proxies for
702 silicate weathering? Earth and Planetary Science Letters 237, 387–401.
703 doi:10.1016/j.epsl.2005.07.019
704 Kısakürek, B., Widdowson, M., James, R.H., 2004. Behaviour of Li isotopes during continental
705 weathering: the Bidar laterite profile, India. Chemical Geology 212, 27–44.
706 doi:10.1016/j.chemgeo.2004.08.027
707 Langmuir, C.H., Vocke, R.D., Jr, Hanson, G.N., Hart, S.R., 1978. A general mixing equation with
708 applications to Icelandic basalts. Earth and Planetary Science Letters 37, 380–392.
709 Lee, C.-T.A., Morton, D.M., Little, M.G., Kistler, R., Horodyskyj, U.N., Leeman, W.P., Agranier,
710 A., 2008. Regulating continent growth and composition by chemical weathering.
711 Proceedings of the National Academy of Sciences 105, 4981–4986.
712 doi:10.1073/pna5.0711143105

713 Liu, T.S., 1985. Loess and the Environment. China Ocean Press, Beijing.
714 Liu, X.-M., Rudnick, R.L., 2011. Constraints on continental crustal mass loss via chemical
715 weathering using lithium and its isotopes. Proceedings of the National Academy of Sciences
716 108, 20873–20880. doi:10.1073/pnas.1115671108
717 Liu, X.-M., Rudnick, R.L., Hier-Majumder, S., Sirbescu, M.-L.C., 2010. Processes controlling
718 lithium isotopic distribution in contact aureoles: A case study of the Florence County
719 pegmatites, Wisconsin. Geochem. Geophys. Geosyst. 11. doi:10.1029/2010GC003063
720 Liu, X.-M., Rudnick, R.L., McDonough, W.F., Cummings, M.L., 2013. Influence of chemical
721 weathering on the compositionof the continental crust: Insights from Li and Nd isotopesin
722 bauxite profiles developed on Columbia River Basalts. Geochimica et Cosmochimica Acta
723 115, 73–91. doi:10.1016/j.gca.2013.03.043
724 Liu, X.-M., Wanner, C., Rudnick, R.L., McDonough, W.F., 2015. Processes controlling δ7Li in
725 rivers illuminated by study of streams and groundwaters draining basalts. Earth and
726 Planetary Science Letters 409, 212–224. doi:10.1016/j.epsl.2014.10.032
727 Lynton, S.J., Walker, R.J., Candela, P.A., 2005. Lithium isotopes in the system Qz-Ms-fluid:An
728 experimental study. Geochimica et Cosmochimica Acta 69, 3337–3347.
729 doi:10.1016/j.gca.2005.02.009
730 Maloney, J.S., Nabelek, P.I., 2008. Lithium and its isotopes in tourmaline as indicators of the
731 crystallization process in the San Diego County pegmatites, California, USA. European
732 Journal of Mineralogy.
733 Magna, T., Wiechert, U.H., Halliday, A.N., 2004. Low-blank isotope ratio measurement of small
734 samples of lithium using multiple-collector ICPMS. International Journal of Mass
735 Spectrometry 239, 67–76. doi:10.1016/j.ijms.2004.09.008
736 Marks, M.A., Rudnick, R.L., Ludwig, T., Marschall, H., Zack, T., Halama, R., McDonough, W.F.,
737 Rost, D., Wenzel, T., Vicenzi, E.P., 2008. Sodic pyroxene and sodic amphibole as potential
738 reference materials for in situ lithium isotope determinations by SIMS. Geostandards and
739 Geoanalytical Research 32, 295–310.
740 McLennan, S.M., 2001. Relationships between the trace element composition of sedimentary
741 rocks and upper continental crust. Geochem. Geophys. Geosyst. 2, art. no. 2000GC000109.
742 McLennan, S.M., Hemming, S., McDaniel, D.K., Hanson, G.N., 1993. Geochemical approaches
743 to sedimentation, provenance, and tectonics. Special Papers-Geological Society of America
744 21–21.
745 Meybeck, M., 1987. Global chemical weathering of surficial rocks estimated from river dissolved
746 loads. American Journal of Science 287, 401–428.

747 Millot, R., Vigier, N., Gaillardet, J., 2010. Behaviour of lithium and its isotopes during weathering
748 in the Mackenzie Basin, Canada. Geochimica et Cosmochimica Acta 74, 3897–3912.
749 doi:10.1016/j.gca.2010.04.025
750 Monecke, T., Bombach, G., Klemm, W., Kempe, U., GOTZE, J., Wolf, D., 2000. Determination of
751 trace elements in the quartz reference material UNS-SpS and in natural quartz samples by
752 ICP-MS. Geostandards Newsletter-the Journal of Geostandards and Geoanalysis 24, 73–
753 81.
754 Moriguti, T., Nakamura, E., 1998a. High-yield lithium separation and the precise isotopic
755 analysis for natural rock and aqueous samples. Chemical Geology 145, 91–104.
756 Moriguti, T., Nakamura, E., 1998b. Across-arc variation of Li isotopes in lavas and implications
757 for crust/mantle recycling at subduction zones. Earth and Planetary Science Letters.
758 doi:10.1016/S0012-821X(98)00184-8
759 Nesbitt, H.W., Young, G.M., 1982. Early Proterozoic Climates and Plate Motions Inferred From
760 Major Element Chemistry of Lutites. Nature 299, 715–717.
761 Peucker Ehrenbrink, B., Jahn, B.-M., 2001. Rhenium-osmium isotope systematics and platinum
762 group element concentrations: Loess and the upper continental crust. Geochem. Geophys.
763 Geosyst. 2.
764 Pécsi, M., 1990. Loess is not just the accumulation of dust. Quaternary International 7, 1–21.
765 Pistiner, J.S., Henderson, G.M., 2003. Lithium-isotope fractionation during continental
766 weathering processes. Earth and Planetary Science Letters 214, 327–339.
767 doi:10.1016/S0012-821X(03)00348-0
768 Plank, T., 2005. Constraints from Thorium/Lanthanum on Sediment Recycling at Subduction
769 Zones and the Evolution of the Continents. Journal of Petrology 46, 921–944.
770 doi:10.1093/petrology/egi005
771 Pye, K., 1995. The nature, origin and accumulation of loess. Quaternary Science Reviews 14,
772 653–667.
773 Qiu, L., Rudnick, R.L., Ague, J.J., McDonough, W.F., 2011. A lithium isotopic study of sub-
774 greenschist to greenschist facies metamorphism in an accretionary prism, New Zealand.
775 Earth and Planetary Science Letters 301, 213–221. doi:10.1016/j.epsl.2010.11.001
776 Qiu, L., Rudnick, R.L., McDonough, W.F., Merriman, R.J., 2009. Li in mudrocks from the British
777 Caledonides: Metamorphism and source influences. Geochimica et Cosmochimica Acta 73,
778 7325–7340. doi:10.1016/j.gca.2009.08.017
779 Romer, R.L., Meixner, A., Hahne, K., 2014. Lithium and boron isotopic composition of
780 sedimentary rocks - The role of source history and depositional environment: A 250 Ma

781 record from the Cadomian orogeny to the Variscan orogeny. Gondwana Research 26,
782 1093–1110. doi:10.1016/j.gr.2013.08.015
783 Rousseau, D.-D., Chauvel, C., Sima, A., Hatté, C., Lagroix, F., Antoine, P., Balkanski, Y., Fuchs,
784 M., Mellett, C., Kageyama, M., Ramstein, G., Lang, A., 2014. European glacial dust
785 deposits: Geochemical constraints on atmospheric dust cycle modeling. Geophysical
786 Reasearch Letters 41, 7666–7674. doi:10.1002/(ISSN)1944-8007
787 Rousseau, D.D., Derbyshire, E., Antoine, P., Hatté, C., 2007. Loess Records Europe, in:
788 Encyclopedia of Quaternary Science (Second Edition). Elsevier, pp. 606–619.
789 Rudnick, R.L., 1995. Making continental crust. Nature 378, 571–577.
790 Rudnick, R.L., Gao, S., 2014. 4.1 Composition of the Continental Crust, 2nd ed, Treatise on
791 Geochemistry. Elsevier Ltd. doi:10.1016/B978-0-08-095975-7.00301-6
792 Rudnick, R.L., Tomascak, P.B., Njo, H.B., Gardner, L.R., 2004. Extreme lithium isotopic
793 fractionation during continental weathering revealed in saprolites from South Carolina.
794 Chemical Geology 212, 45–57. doi:10.1016/j.chemgeo.2004.08.008
795 Ryan, J.G., Langmuir, C.H., 1987. The systematics of lithium abundances in young volcanic
796 rocks. Geochimica et Cosmochimica Acta 51, 1727–1741.
797 Seitz, H.-M., Brey, G.P., Lahaye, Y., Durali, S., Weyer, S., 2004. Lithium isotopic signatures of
798 peridotite xenoliths and isotopic fractionation at high temperature between olivine and
799 pyroxenes. Chemical Geology 212, 163–177. doi:10.1016/j.chemgeo.2004.08.009
800 Shaw, D.M., Dostal, J., Keays, R.R., 1976. Additional estimates of continental surface
801 Precambrian shield composition in Canada. Geochemica and Cosmochimica Acta Vol. 40,
802 73–83.
803 Shaw, D.M., Reilly, G.A., Muysson, J.R., Pattenden, G.E., Campbell, F.E., 1967. An estimate of
804 the chemical composition of the Canadian Precambrian shield. Canadian Journal of Earth
805 Sciences 4, 829–853. doi:10.1139/e67-058
806 Smith, J., Vance, D., Kemp, R.A., Archer, C., Toms, P., King, M., Zárate, M., 2003. Isotopic
807 constraints on the source of Argentinian loess – with implications for atmospheric circulation
808 and the provenance of Antarctic dust during recent glacial maxima. Earth and Planetary
809 Science Letters 212, 181–196. doi:10.1016/S0012-821X(03)00260-7
810 Swineford, A., Frye, J.C., 1955. Petrographic comparison of some loess samples from western
811 Europe with Kansas loess. Journal of Sedimentary Research 25.
812 Tang, M., Rudnick, R.L., Chauvel, C., 2014. Sedimentary input to the source of Lesser Antilles
813 lavas: A Li perspective. Geochimica et Cosmochimica Acta 144, 43–58.
814 doi:10.1016/j.gca.2014.09.003

Taylor, S.R., McLennan, S.M., 1985. The continental crust: Its composition and evolution. Blackwell Scientific Pub.,Palo Alto, CA.

Taylor, S.R., McLennan, S.M., McCulloch, M.T., 1983. Geochemistry of Loess, Continental Crustal Composition and Crustal Model Ages. Geochimica et Cosmochimica Acta 47, 1897–1905.

Teng, F.-Z., Rudnick, R.L., McDonough, W.F., Gao, S., Tomascak, P.B., Liu, Y., 2008. Lithium isotopic composition and concentration of the deep continental crust. Chemical Geology 255, 47–59. doi:10.1016/j.chemgeo.2008.06.009

Teng, F.Z., McDonough, W.F., Rudnick, R.L., Dalpé, C., Tomascak, P.B., Chappell, B.W., Gao, S., 2004. Lithium isotopic composition and concentration of the upper continental crust. Geochimica et Cosmochimica Acta 68, 4167–4178. doi:10.1016/j.gca.2004.03.031

Teng, F.Z., McDonough, W.F., Rudnick, R.L., Walker, R.J., Sirbescu, M.L.C., 2006. Lithium isotopic systematics of granites and pegmatites from the Black Hills, South Dakota. American Mineralogist 91, 1488–1498. doi:10.2138/am.2006.2083

Teng, F.Z., McDonough, W.F., Rudnick, R.L., Wing, B., 2007. Limited lithium isotopic fractionation during progressive metamorphic dehydration in metapelites: A case study from the Onawa contact aureole, Maine. Chemical Geology 239, 1–12. doi:10.1016/j.chemgeo.2006.12.003

Teruggi, M.E., 1957. The nature and origin of Argentine loess. Journal of Sedimentary Research 27.

Thirumalai, K., Singh, A., Ramesh, R., 2011. A MATLAB™ code to perform weighted linear regression with (correlated or uncorrelated) errors in bivariate data. Journal of the Geological Society of India 77, 377–380.

Tomascak, P.B., Langmuir, C.H., le Roux, P.J., Shirey, S.B., 2008. Lithium isotopes in global mid-ocean ridge basalts. Geochimica et Cosmochimica Acta 72, 1626–1637. doi:10.1016/j.gca.2007.12.021

Tomascak, P.B., Tera, F., Helz, R.T., Walker, R.J., 1999. The absence of lithium isotope fractionation during basalt differentiation: new measurements by multicollector sector ICP-MS. Geochimica et Cosmochimica Acta 63, 907–910.

Tsai, P.-H., You, C.-F., Huang, K.-F., Chung, C.-H., Sun, Y.-B., 2014. Lithium distribution and isotopic fractionation during chemical weathering and soil formation in a loess profile. Journal of Asian Earth Sciences 87, 1–10. doi:10.1016/j.jseaes.2014.02.001

Ushikubo, T., Kita, N.T., Cavosie, A.J., Wilde, S.A., Rudnick, R.L., Valley, J.W., 2008. Lithium in Jack Hills zircons: Evidence for extensive weathering of Earth's earliest crust. Earth and

Planetary Science Letters 272, 666–676. doi:10.1016/j.epsl.2008.05.032
Vigier, N., Decarreau, A., Millot, R., Carignan, J., Petit, S., France-Lanord, C., 2008. Quantifying Li isotope fractionation during smectite formation and implications for the Li cycle. Geochimica et Cosmochimica Acta 72, 780–792. doi:10.1016/j.gca.2007.11.011
Vlastélic, I., Staudacher, T., Bachèlery, P., Télouk, P., Neuville, D., Benbakkar, M., 2011. Lithium isotope fractionation during magma degassing: Constraints from silicic differentiates and natural gas condensates from Piton de la Fournaise volcano (Réunion Island). Chemical Geology 284, 26–34. doi:10.1016/j.chemgeo.2011.02.002
Yang, S., Ding, F., Ding, Z., 2006. Pleistocene chemical weathering history of Asian arid and semi-arid regions recorded in loess deposits of China and Tajikistan. Geochimica et Cosmochimica Acta 70, 1695–1709. doi:10.1016/j.gca.2005.12.012
Yang, S.L., Ding, Z.L., 2004. Comparison of particle size characteristics of the Tertiary 'red clay' and Pleistocene loess in the Chinese Loess Plateau: implications for origin and sources of the “red clay.” Sedimentology 51, 77–93. doi:10.1046/j.1365-3091.2003.00612.x
York, D., Evensen, N.M., Martínez, M.L., De Basabe Delgado, J., 2004. Unified equations for the slope, intercept, and standard errors of the best straight line. Am. J. Phys. 72, 367. doi:10.1119/1.1632486
Zárate, M., 2003. Loess of southern South America. Quaternary Science Reviews 22, 1987–2006. doi:10.1016/S0277-3791(03)00165-3

Highlights

- Desert loesses are good proxies to average Li composition of UCC
- δ^7Li and Li concentrations are controlled by mineralogical sorting
- New and more precise average δ^7Li and Li concentration for the UCC
- Quantification of the degree of weathering experienced by the UCC

Figure 1

Figure 1

Click here to download Figure: Figure 1.pdf

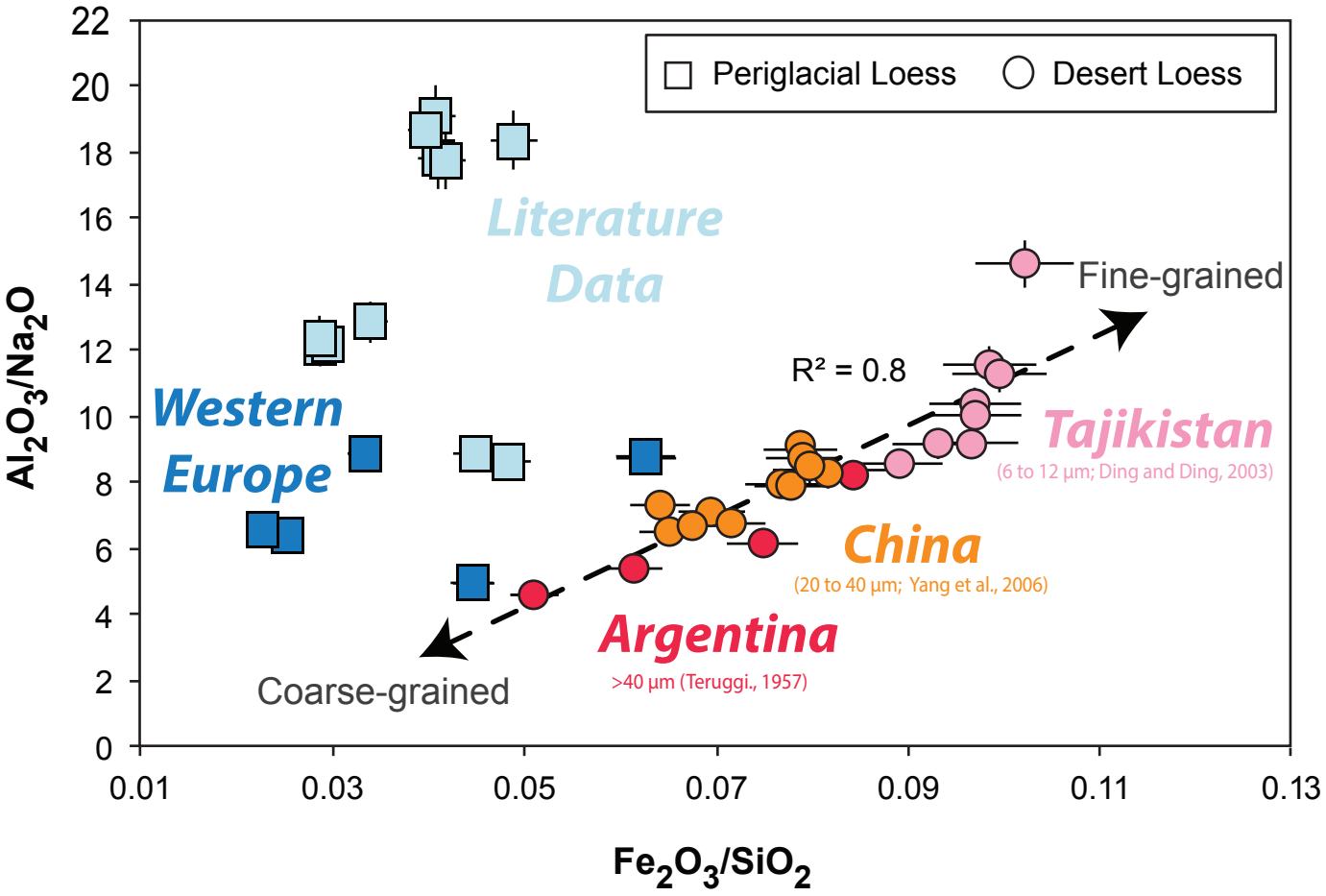

Figure 2
Figure 2
Click here to download Figure: Figure 2.pdf

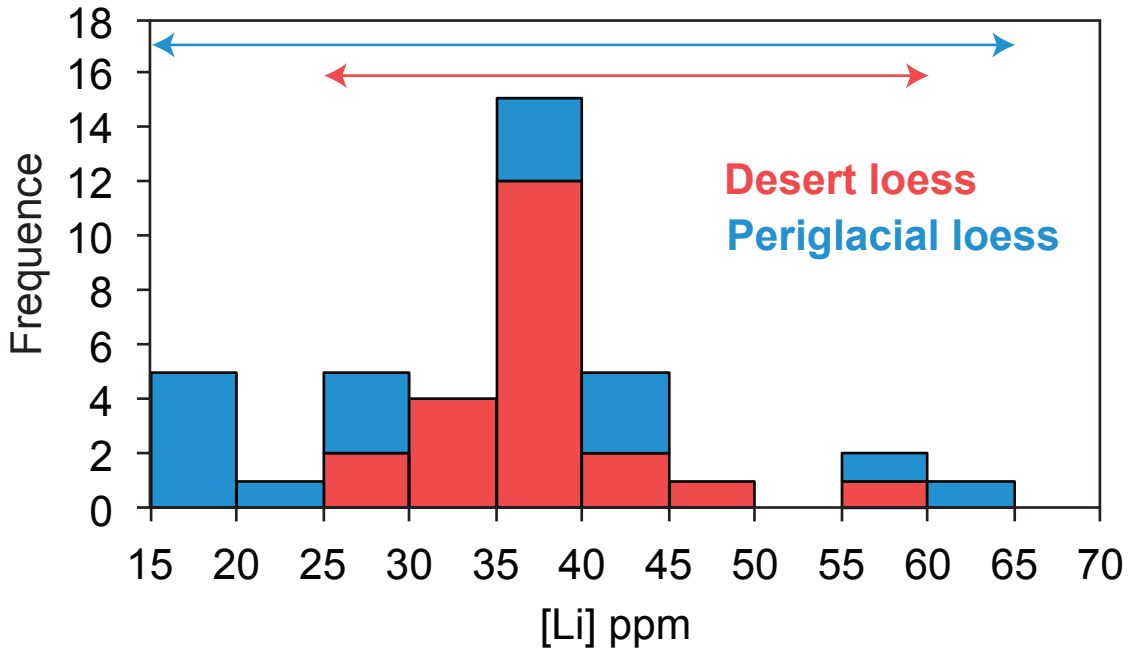

Figure 3
Figure 3
Click here to download Figure: Figure 3.pdf

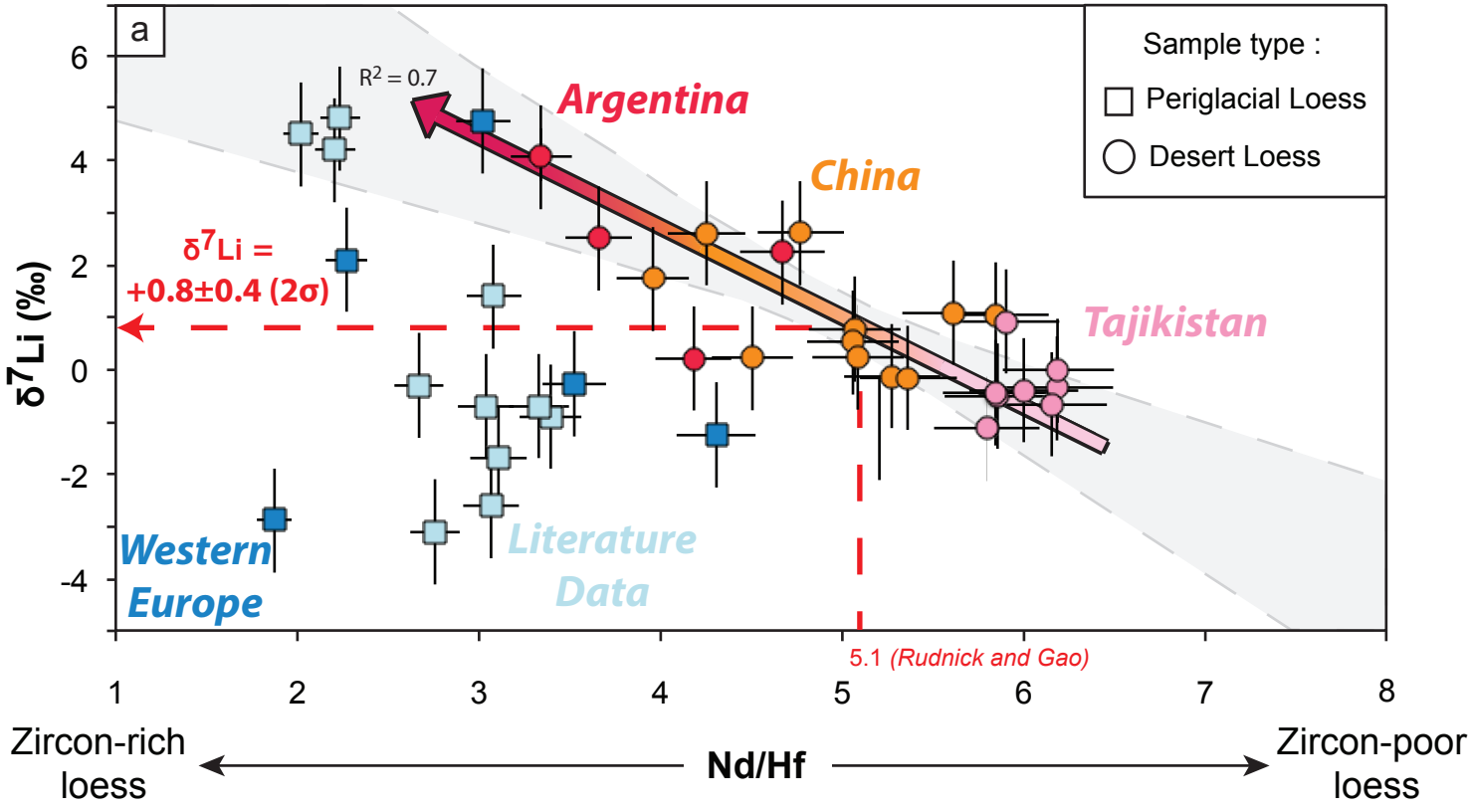

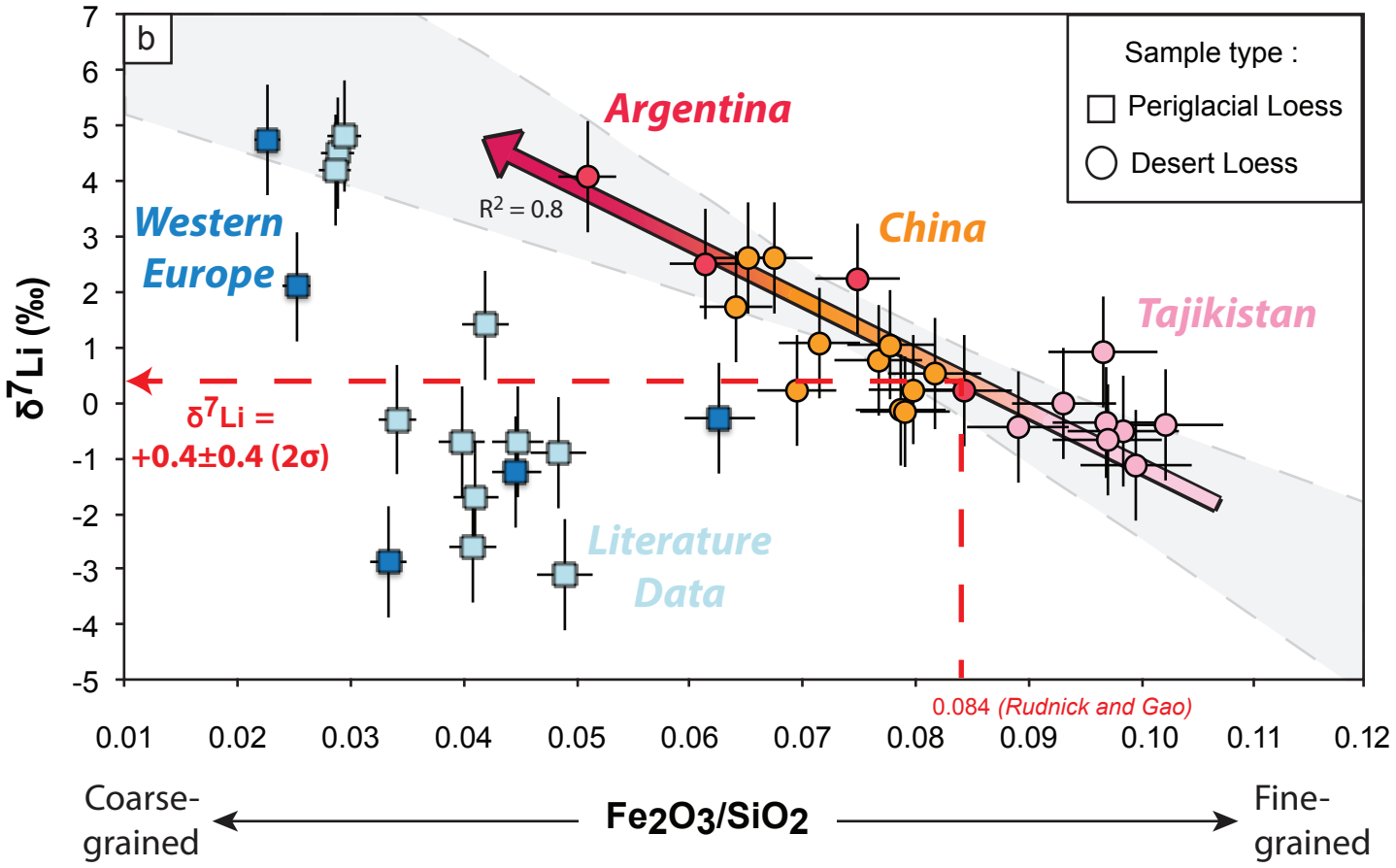

Figure 4

Click here to download Figure: Figure 4.pdf

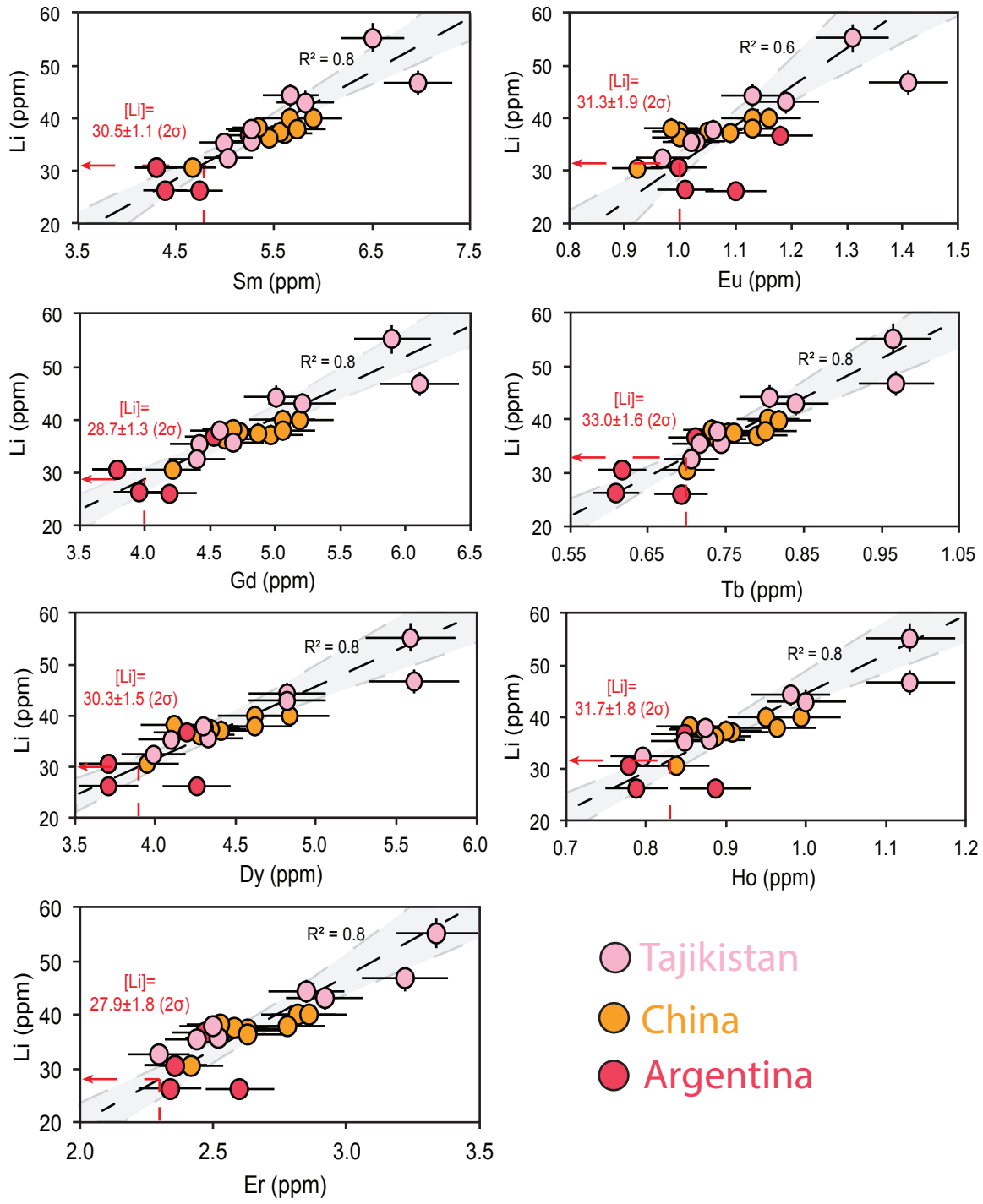

Figure 5
Figure 5
Click here to download Figure: Figure 5.pdf

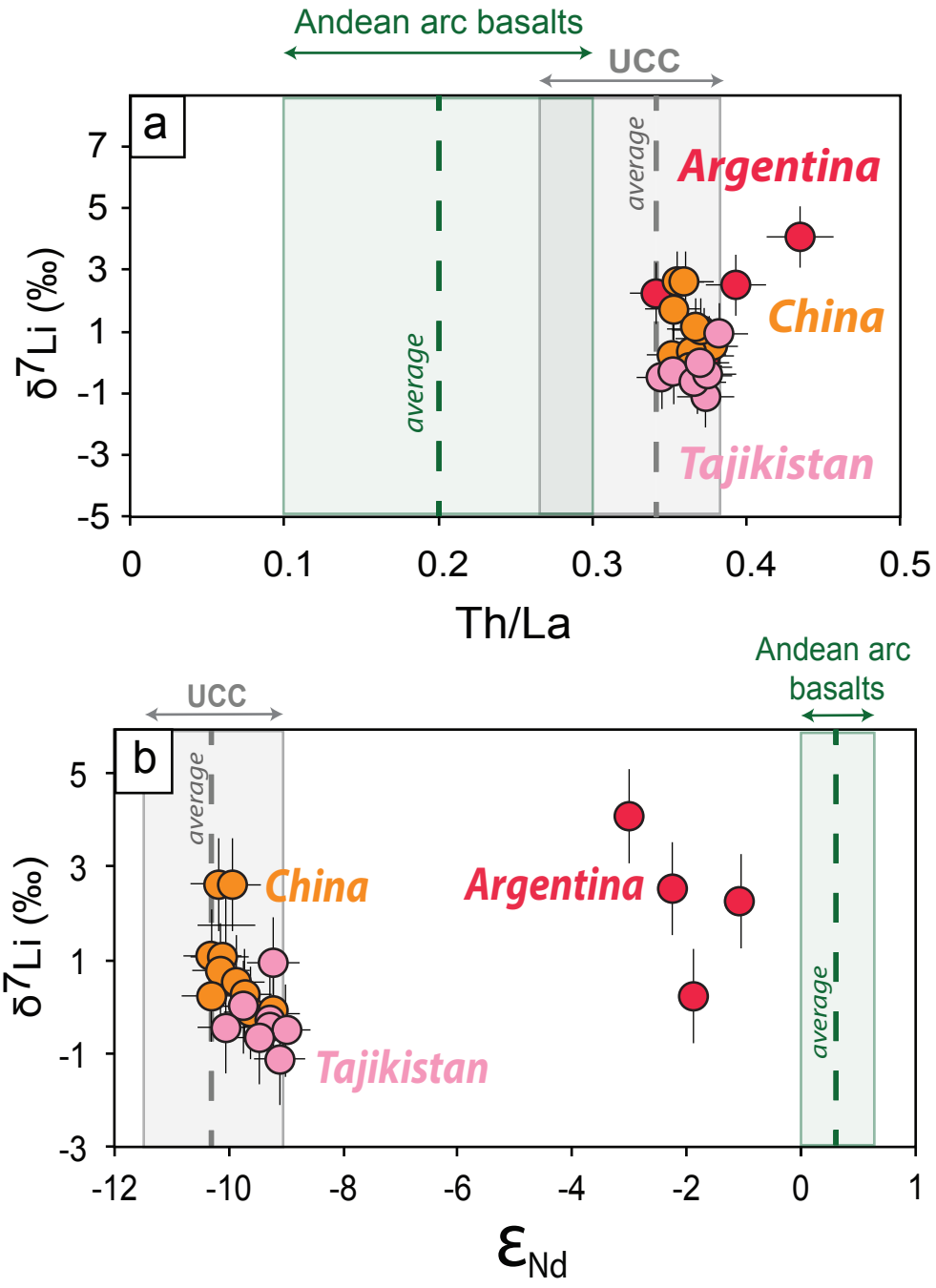

Figure 6

Figure 6

Click here to download Figure: Figure 6.pdf

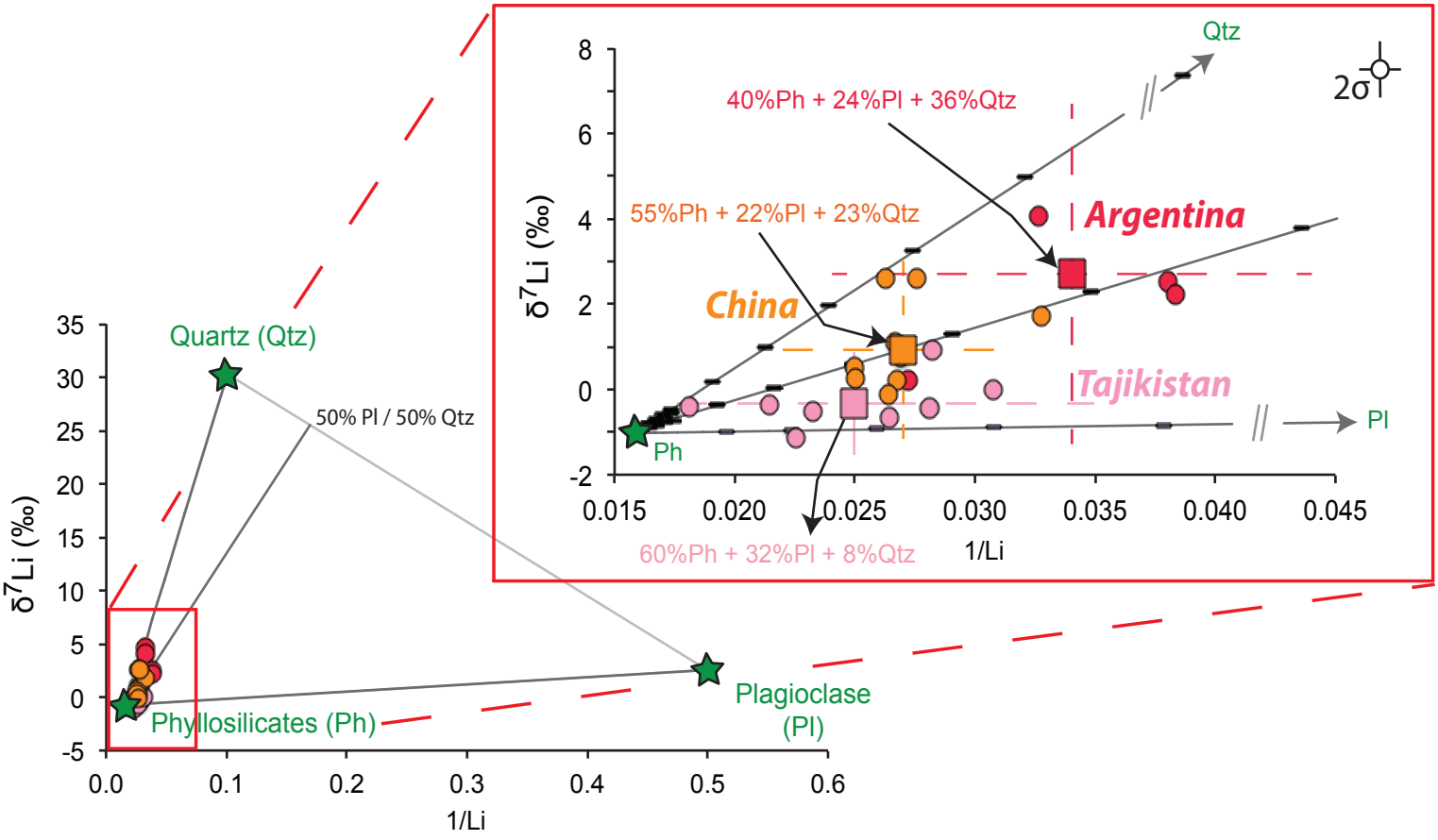

Figure 7

Figure 7

Click here to download Figure: Figure 7.pdf

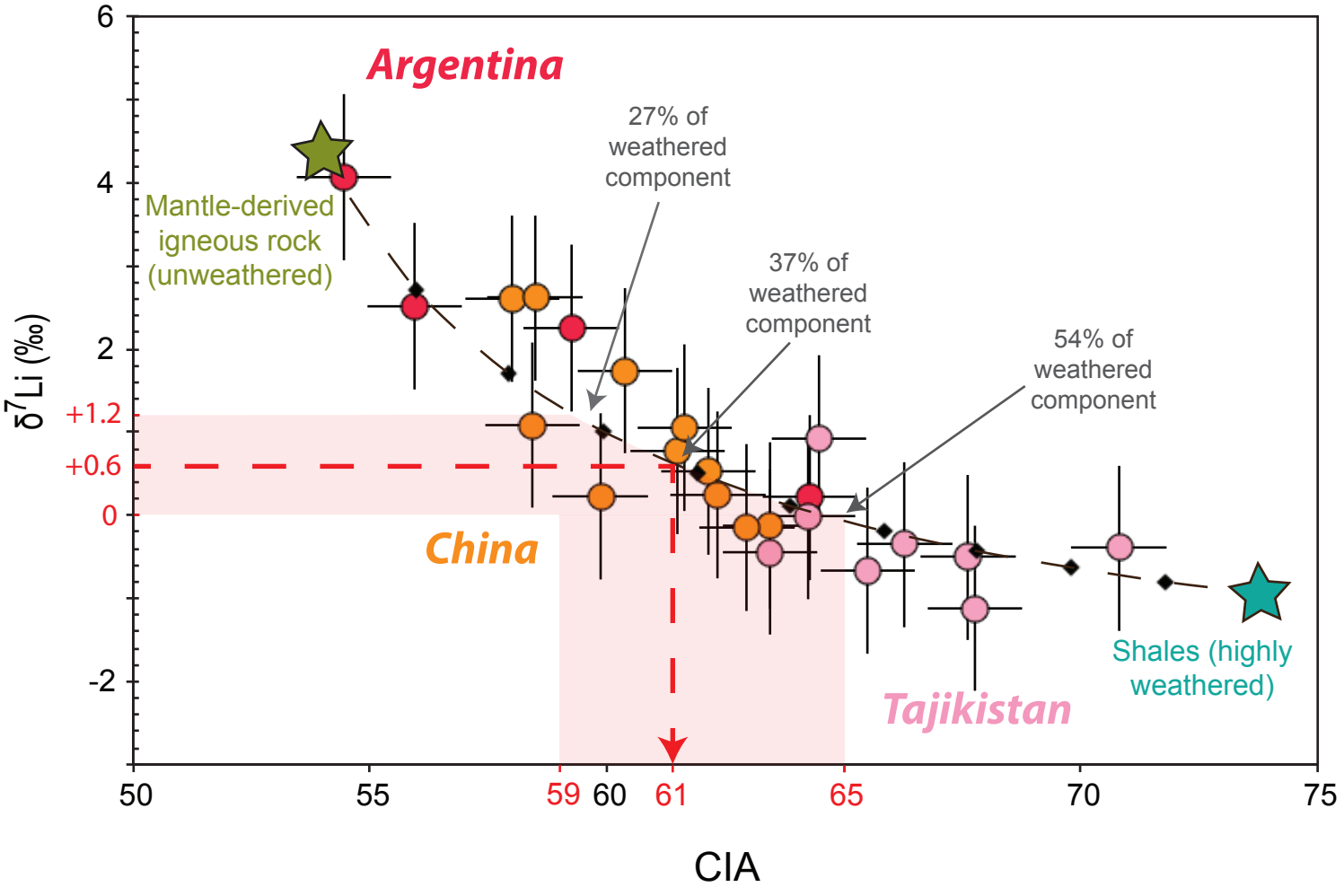

Table 1
Click here to download Table: Table 1.xlsx

Table 1

Sample name	Location	Longitude	Latitude	δ^7Li* (‰)	[Li]** (ppm)
Western Europe (Periglacial loess)					
PR RT	Port Racine, Normandy, France	1°53'W	49°4'3N	2.1	17.9
SAB 1a <160 mm	Sables d'or, France	2°24'W	48°37'N	4.7	16.6
LO94	Spitsbergen (Svalbard)	20°43'E	77°40'N	-1.2	61.3
P2E1	Spitsbergen (Svalbard)			-0.3	59.9
SCIL	Scilly Island, England	6°20'W	49°55'N	-2.9	41.1
SCIL dup	Scilly Island, England			-1.5	
China (Desert loess)					
JX-4	Jixian			0.8	37.1
JX-6	Jixian	110°39'E	36°06'N	0.2	37.4
JX-10	Jixian			1.7	30.5
XF-10	Xifeng	107°42'E	35°45'N	0.5	40
XF-6	Xifeng			0.2	39.9
XN-2	Xining			1.1	37.5
XN-4	Xining	101°48'E	36°36'N	2.6	36.3
XN-10	Xining			2.6	38.1
L9	Luochuan			-0.1	37.9
L6	Luochuan	109°26'E	35°28'N	-0.2	no data
L2	Luochuan			1.1	no data
Tajikistan (Desert loess)					
TJK2772	Tajikistan			-1.1	44.3
TJK2773	Tajikistan			-0.5	43.0
TJK2930	Tajikistan			-0.4	35.6
TJK3012	Tajikistan	69°49'57"E	38°23'32"N	-0.4	46.7
TJK3070	Tajikistan			0.9	35.4
TJK3148	Tajikistan			-0.7	37.8
TJK3179	Tajikistan			-0.4	55.2
TJK3198	Tajikistan			0.0	32.5
Argentina (Desert loess)					
12-14	Argentina			2.5	26.3
24-26	Argentina			2.2	26.1
40RT	Argentina	59°22'W	34°38'S	0.2	36.7
LUJA	Argentina			4.1	30.6
LUJA dup	Argentina			4.6	